

Available online at www.sciencedirect.com

ScienceDirect





www.materialstoday.com/proceedings

SACT 2016

Structures and properties of N-doped TiO₂ nanotubes arrays synthesized by the anodization method for hydrogen production

N. Kodtharin^a, R. Vongwatthaporn^a, J. Nutariya^a, C. Sricheewin^b, E.N. Timah^c, K. Sivalertporn^a, O. Thumthan^a, U. Tipparach^{a,*}

^aDepartment of Physics, Faculty of Science, Ubon Ratchathani University, Ubon Ratchathani 34190, Thailand ^bDivision of Science bDepartment of Physics, Petchaboon Ratchabhat University, Phetchaboon 67000, Thailand ^cScience Division, Srinakharinwirot University Demonstration School, Soi Sukhumvit 23, Watthana, Bangkok 10110, Thailand

Abstract

The films of TiO_2 nanotube arrays were fabricated by the anodization of Ti metal sheets for photocatalytic hydrogen production. The anodization was carried out in electrolytes prepared by mixing ethylene glycol (EG), ammonium fluoride (0.3 wt % NH_4F) and deionized water (2 Vol % H_2O). DC power supply was used at a constant voltage of 50 Volts. The nanotube arrays were aged in different amounts of ammonia (NH_3) as nitrogen dopants. The morphology of the nanotube arrays was characterized by scanning electron microscopy (SEM). The phase and structure of the TiO_2 nanotube arrays were determined by X-ray diffraction (XRD). The phase of the nanotubes is transformed from anatase to rutile when annealing temperature is changed from 450 °C to 500 °C or higher. The phase of the nanotubes became completely rutile when the nanotube arrays were 700 °C or higher, and the nanotubes were transformed to nanacrystalline. X-ray Photoelectron spectroscopy (XPS) was used to determine the dopant presenting in TiO_2 structure. UV-vis spectroscopy was used to study the optical property of the nanotubes. The diameters of TiO_2 nanotubes were about 200 nm. The highest density of TiO_2 nanotubes was obtained when the nanotubes were doped with 6% by volume of ammonia. The photocatalytic activity was examined without an external applied potential. The maximum photocurrent density was 2.7 mA/cm² under illumination of 100 mW/cm² corresponding with photoconversion efficiency of 3.3%.

Selection and/or Peer-review under responsibility of SACT 2016.

Keywords: Titania (TiO2); anodization; Hydrogen production

^{*} Corresponding author. Tel.: +66+45-288981; fax: +66+45-288381. E-mail address: udom.t@ubu.ac.th

1. Introduction

Titania (TiO₂) nanotube arrays have received a great deal of attention owing to their potential applications in a wide range of fields such as photocatalysts, dye-sensitive solar cells, photochromic devices, gas sensing, and hydrogen production [1-8]. The conversion of sunlight to energy in the forms of electricity or hydrogen is an ultimate goal of scientific and technological interests which solution may be feasible importance as a renewable source of sustainable and environmentally friendly energy for next generations. Photoelectrolysis of water to produce hydrogen (H₂) have attracted attention because it is renewable and environmentally friendly.

The photocatalytic evolution of H_2 and O_2 from water occurs when a photocatalytic agent with appropriate band gap is illuminated by sufficiently energetic light. Honda and Fujishima [1] showed the process of electrochemical photolysis of water using semiconductor TiO_2 . Since then, a large number of semiconductor materials have been employed for photoanodes which are called working anodes for hydrogen production. All of semiconductor materials, TiO_2 and modified structure TiO_2 are widely used because they are highly photocatalytic, stable, abundant, and environmentally sound. However, the wide band gap of TiO_2 limits the absorption of sunlight to the high energy portion in UV of solar spectrum which contains about 4 percent of whole solar energy [9].

It is believed that the band gap of TiO₂ can be reduced by metal-doping and this will result in exploiting more solar spectrum. The photoanodes were in TiO₂ thin films, metal-doped TiO₂ [, and TiO₂ nanotubes [10]. It is also agreed that photoactivity of TiO₂ depends on its crystal structure. The suitable crystal for photocatalysis is anatase TiO₂. However, the revolution of hydrogen may not increase as expected due to electro-hole recombination [11]. To overcome the recombination of electro-hole pairs, research introduced Pt-loaded TiO₂ thin films as a working electrode. In this work, we modified the structure of TiO₂ nanotubes by doping nitrigen to make working electrodes of photoelectrochemical cells (PEC) for hydrogen production and performed photocatalysis test.

2. Experimental procedure

In this research the TiO₂ nanotubes were synthesized by DC anodization at room temperature on titanium sheet of thickness 0.2 mm, of diameter 1 cm and 99.7 % purity, obtained from Sigma Aldrich. Before anodization, the sheet was first polished and ultrasonicated for 10 minutes in isopropanol, de-ionized water and ethanol. The electrolyte solution which consist of ethylene glycol (EG), ammonium fluoride (0.3 % wt NH₄F) and deionized water (2 % vol D.I. H₂O), was stirred magnetically for 2 hours and kept for 5 hours prior to anodization. The system consists of a two-electrode configuration. The anode was Ti substrate mounted onto a home-made housing apparatus to be anodized and the counter electrode was highly pure platinum. The anode and cathode for the electrolysis were Ti and Pt, respectively. This apparatus allows only one face of the titaniun substrate contacts with the electrolyte [12]. The anodization process was carried on under a constant dc potential 50 V for 2 hrs. All substrates were annealed at 450 °C for 2 hrs to obtain anatase crystalline phases of TiO₂. After preparation of the TNTs, the samples were calcinated at 500 °C for 2 hours, and aged in a mixture containing ethanol, 30 % vol D.I. H₂O, and 1M ammonia solution (NH₃) as source of nitrogen. The volume of NH₃ was varied (1 %, 3 %, 6 % and 12 %) and each sample was aged for 10 hours at room temperature. The volume of NH₃ was varied (1 %, 3 %, 6 % and 12 %) and each sample was aged for 10 hours at room temperature. After being aged, the samples were reannealed at 450 °C for 2 hours. Finally, the samples were ultrasonicated and dried in air. To investigate the surface morphology and microstructure of TiO₂ nanotubes, all resultant samples were characterized by SEM, XRD, XPS, and UV-vis spectroscopy techniques. PAR 173 Potentiostat/Galvanstat was used to measure the photocurrent of PEC cells.

3. Results and discussion

The XRD patterns of the anodized samples without annealing are shown in Fig. 1 (pre-annealed). The results show that all peaks belong to Ti metal sheet. Anatase and rutile phases of TiO₂ are not observed. They show amorphous phase of TiO₂. The XRD patterns of the anodized samples after annealing at different temperatures are also shown in Fig. 1 (300 to 700 °C). After annealed from 300 to 450 °C for 2 h, the amorphous TiO₂ transformed to a crystalline anatase phase. No rutile phase is detected. The best-single rutile phase was obtained when the nanotubes were annealed at 450 °C. However, the rutile phase of TiO₂ was introduced besides the anatase when the

annealing temperature was 500 °C or higher. Rutile phase was increased when annealing temperatures were increased. The nanotubes completely became a rutile phase after annealing at 700 °C or higher. This result is in agreement with previous works on TiO_2 sol-gel films done by Tipparach et al. [13] and Li et al. [14].

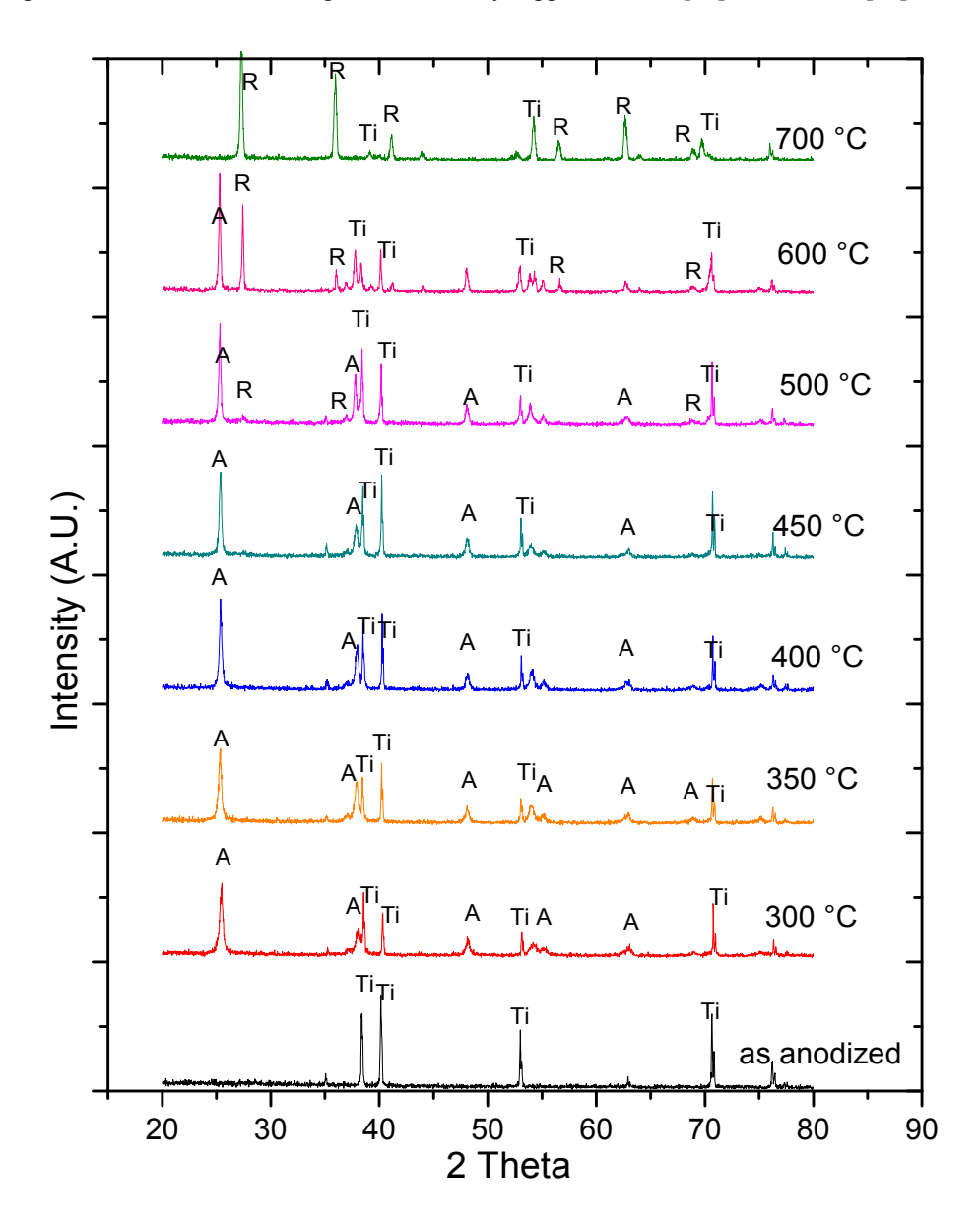


Fig. 1. XRD patterns of as-anodized and annealed TiO_2 nanotube arrays showing amorphous as-anodized and crystalline phases after annealed for 2 hours.

Fig. 3 shows typical SEM images of TiO_2 nanotube arrays. The well-aligned and uniform TiO_2 nanotubes were observed for all anodizing times. It was evident that the TiO_2 nanotubes were small with diameter of about 100-200 nm. The diameter and the density of the nanotubes are likely to be constant when the annealing temperature increased.

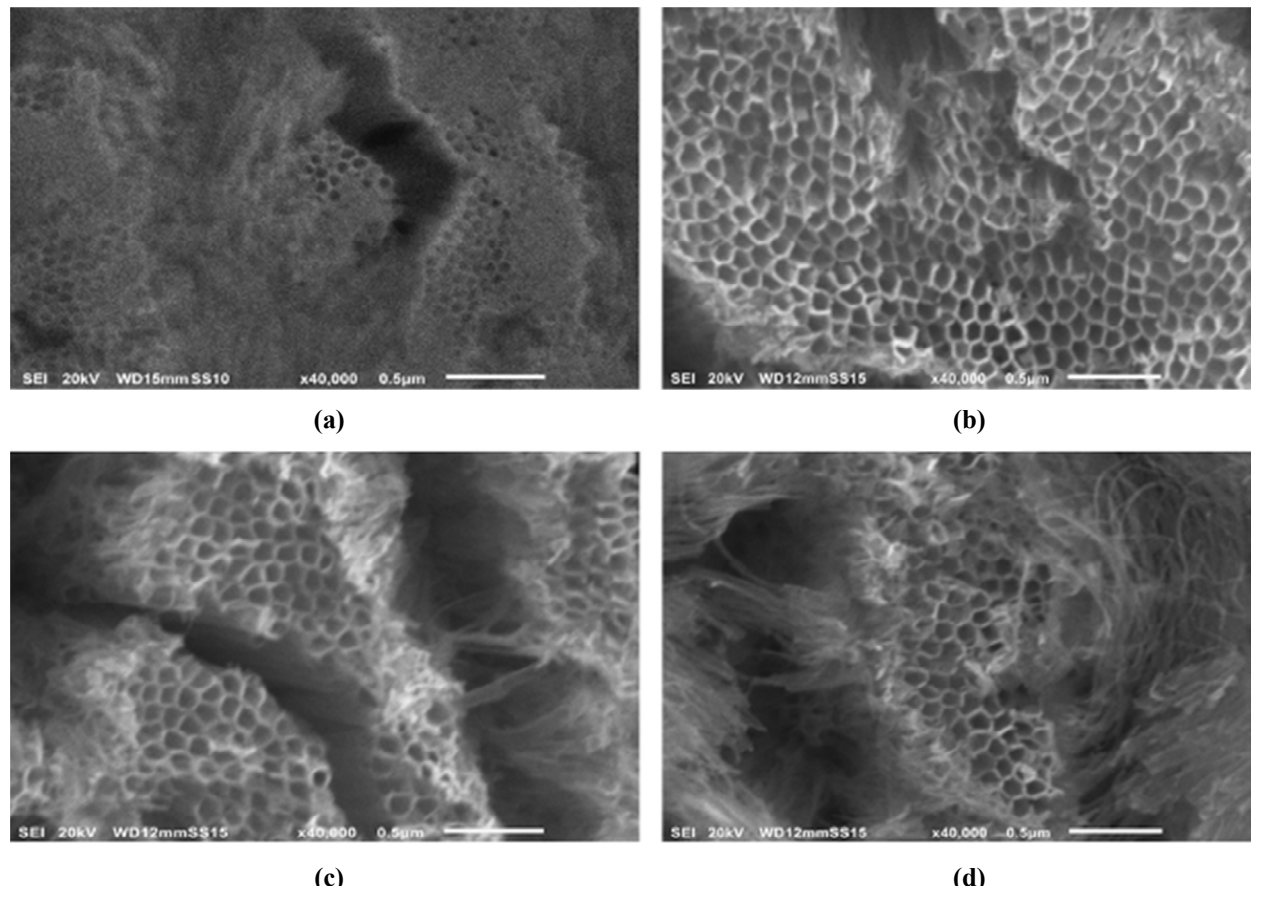


Fig. 2. SEM images of N-doped TiO2 nanotube arrays with different amount of ammonia (a) 1 %, (b) 3 %, (c) 6 % and (d) 12 % by volume.

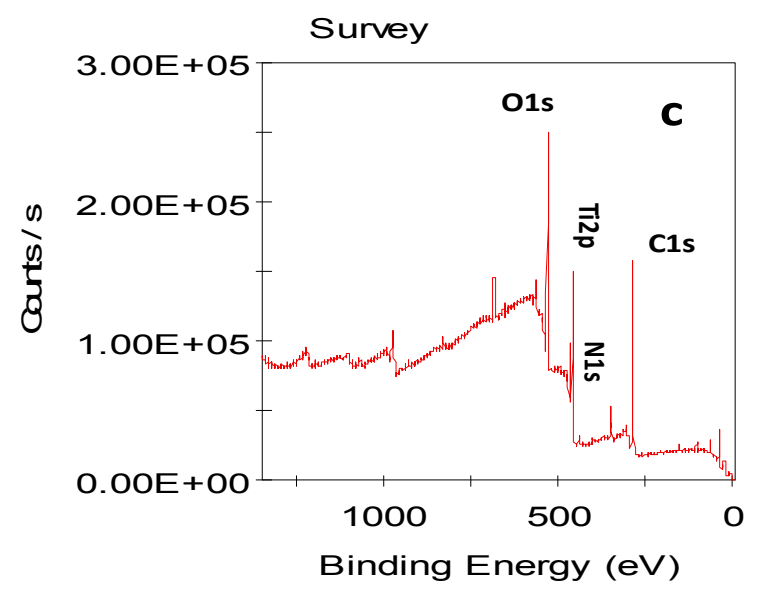


Fig. 3. XPS spectra survey of N-doped TiO_2 nanotube arrays with 6 % vol ammonia.

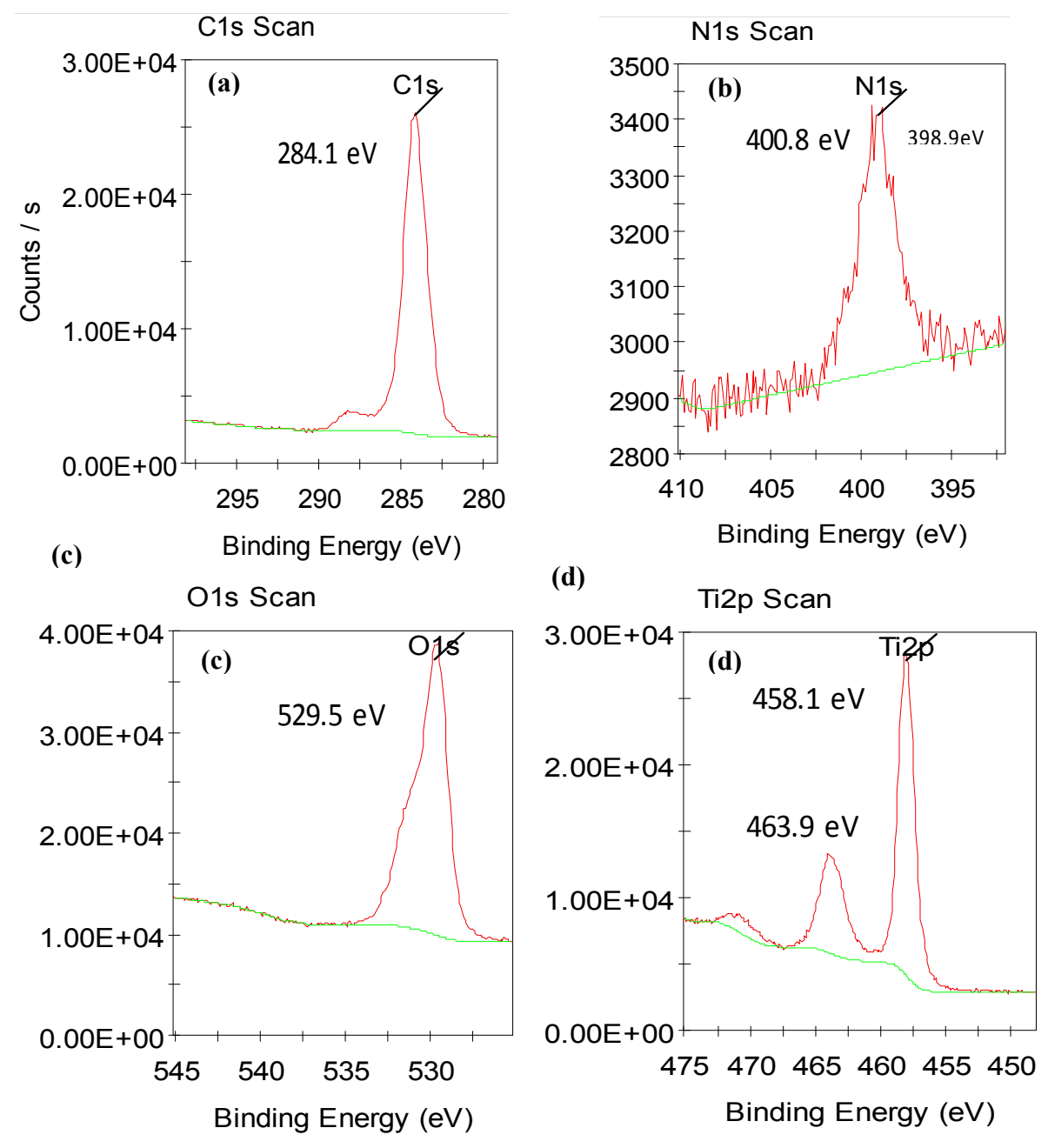


Fig. 4. High resolution XPS spectra scan of N-doped TiO2 nanotube arrays with 6 % vol ammonia.

XPS spectra survey in Fig. 3 confirms the presence of nitrogen, whose percentage increased with the amount of ammonia. Fig. 4 (a)-(d) shows XPS spectra scans for N-doped TiO_2 nanotubes with 6 % vol of ammonia with the obvious C_{1s} , O_{1s} , Ti_{2p} , N_{1s} peaks. The C_{1s} peak that appears at 284.1 eV can be due to pollution of hydrocarbon from the XPS instrument. The XPS spectrum of O_{1s} shows a peak at 529.5 eV which can be attributed to the Ti-O bond [15]. The peaks at 458.1 eV and 463.9 eV corresponds to the Ti_{2p} (1/2) and Ti_{2p} (3/2) electron binding energies, respectively. They could be due to substitution of oxygen atoms by nitrogen atoms, resulting in the formation of O-Ti-N bonds [16]. Both peaks indicate that Ti is present in the Ti^{4+} oxidation state [17, 15]. For pure TiO_2 , the Ti_{2p} characteristic peaks are positioned at 458.5 eV and 464.2 eV, which indicates a small shift when compared to the N-

doped samples. The N_{1s} scan reveals the peaks located at 398.9 eV, and 400.8 eV. The 398.9 eV peak can be attributed to the substitutional Ti-N nitride bond. The N_{1s} 400.8 eV peak can be assigned to the Ti-N-O bonds.

The UVS spectra in Fig. 5 shows that as the amount of ammonia increases, the absorption edge shifts from shorter to longer wavelengths, and the optical band gap reduces from 3.15 eV (at 1 % vol NH₃) to 2.85 eV (at 12 % vol NH₃). This could be due to increase in percentage of the nitrogen and the formation of mid band gaps [4, 17]. A band gap of 2.85 eV corresponds to a red shift in light absorption into the visible region with wavelength 435 nm.

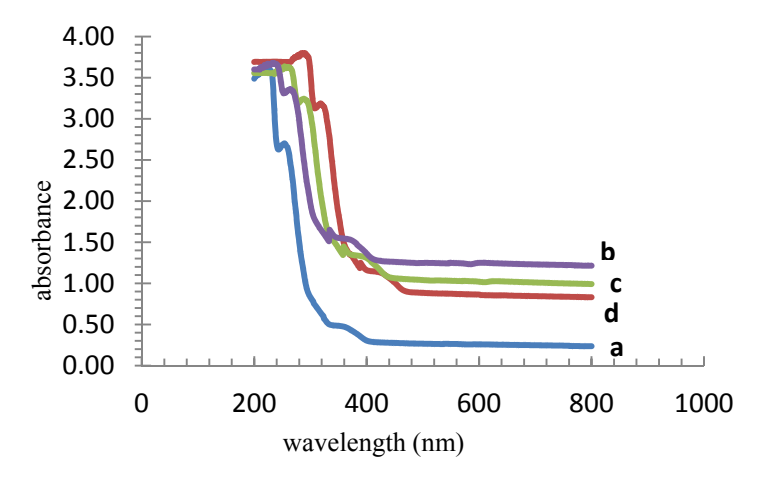


Fig. 5. Te UVS spectra of samples.

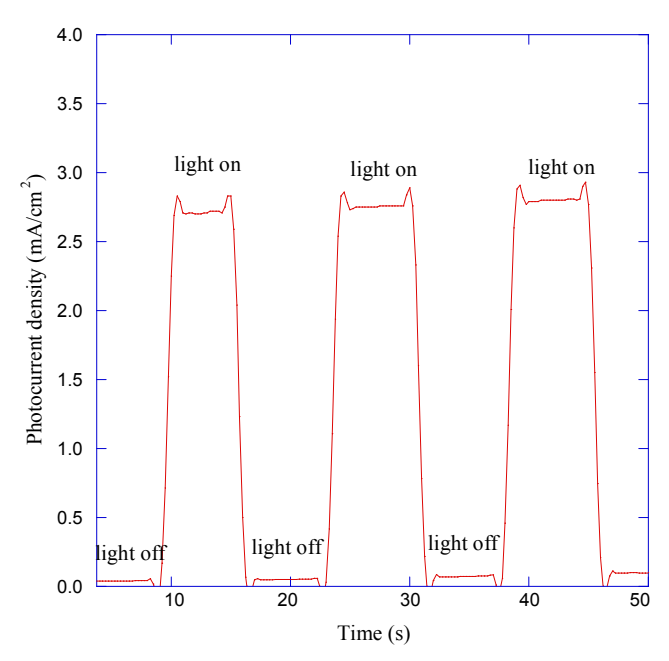


Fig. 6. photocurrent response of samples.

Photoconversion efficiency of TiO₂ nanotube arrays was measured by a standard three-electrode cell at room temperature under the illumination of 100 mW/cm² in a 1 M KOH solution. The photocurrent response measurement was tested without external applied potential to investigate the photoinduced charge separation efficiency of the prepared photanodes and are shown in Fig. 6. When the light was turned on and irradiated the photoanode, the photocurrent rose up and kept constant during the light was on while the light was turned off, the

photocurrent abruptly disappeared. This evident showed that the current came from the illumination. The photoconversion efficiency (η %) of water electrolysis was calculated based on the following relations [19-20],

$$\eta(\%) = \left(\frac{J \times E_{rev}^0}{P_{in}}\right) \times 100,$$

where J is the photocurrent density, $J \times E_{rev}^0$ is the total power output and P_{in} is the power density of incident light and E_{rev}^0 is the standard reversible potential which is 1.23V. The hightest photocurrent density was obtained when the photocurrent density after the switch was used as a working electrode. Without an external bias voltage, the photocurrent density after the switch was turned on was about 3.0 mA/cm² coresponding with the photocoversion efficiency of 3.7 %

This photoconversion efficiency (3.7 %) of TiO₂ nanotube array photoanode is larger than that (0.8%) of nano-TiO₂ particle photoanodes made by sol-gel dip coating films [21]. The increase of photoconversion efficiency may be resulted from the fact that the surface areas of TiO₂ NTs are larger than those of nano-TiO₂ films due to the agglomeration of the small spherical crystals of nano TiO₂ crystals by nature [13]. Another reason may be due to the reduction of TiO₂ nanotubes optical bandgap energy because nitrogen atoms from NH₄F used for making the electrolyte and aging nitrogen (NH₃) incorporate the structure of TiO₂ nanotubes as XPS data show. Decreasing the bandgap energy of TiO₂ leads to increase the utilization of sunlight spectrums and also increase photoactivity.

4. Conclusion

We have synthesized pure and N-doped TiO_2 nanotube arrays on Ti sheet by anodization method in the mixture electrolyte. The post anodization process was carried out by anneaing in air at 450 °C for 2 hrs and aging in the solution in the present of nitrogen (NH₃) with different amounts of ammonia. The mixtures electrolyte was ethylene glycol (EG), ammonium fluoride (0.3 wt % NH₄F) and deionized water (2 Vol % H₂O). The nanotubes are well arraged and the diameters are about 100-200 nm. The photocurrent response indicated that the photocurrent was the contribution of light irradiation on photoanode. The hydrogen can be produced with overall the photoconversion efficiency of 3.3 % when 6% Vol N-doped TiO_2 nanotitania arrays was used as a working electrode for PEC. This photo activity increases because the optical band gap decreases due to nitrogen incorporation in to nanotube structure as confirmed by XPS data.

Acknowledgements

We would like to thank National Research Council of Thailand and Ubon Ratchathani University for financial supports.

References

- [1] A. Fujishima, K. Honda, Nature 238, 1972, 37.
- [2] M. Gra"tzel, Nature 414, 2001, 338.
- [3] C.J. Barbe, F. Arendse, P. Comte, M. Jirousek, F. Lenzmann, V. Shklover, M. Gra"tzel, J. Am. Ceram. Soc. 80, 1997, 3157.
- [4] B. O'Regan, M.A. Gra"tzel, Nature 353, 1991, 737.
- [5] X. Chen, S.S. Mao, Chem. Rev. 107, 2007, 2891.
- [6] E.A. Rozhkova, I. Ulasov, B. Lai, N.M. Dimitrijevic, M.S. Lesniak, T.A. Rajh, Nano Lett. 9 (2009) 3337.
- [7] D. Wang, D. Choi, J. Li, Z. Yang, Z. Nie, R. Kou, D. Hu, C. Wang, L.V. Saraf, J. Zhang, I.A. Aksay, J. Liu, ACS Nano 3 (2009) 907.
- [8] Rinnatha Vongwatthaporn, Narongsak Kodtharin, and Udom Tipparach. Advanced Materials Research. 2015, 1105.
- [9] Bak, T., Nowotny, J., Rekas, M. and Sorrell, C.C, International journal of hydrogen energy, 27(10), 2002, 991.
- [10] Mor GK, Varghese OK, Paulose M, Shankar K, Grimes CA., Solar Energy Materials and Solar Cells. 90(14) 2006, 2011.
- [11] M. Ni, K.H. Michael Leung, Y.C. Dennis Leung, and K. Sumathy, Renewable and Sustainable Energy Reviews, 11(2007) 401.
- [12] Wantawee S, Krongkitsiri P, Saipin T, Samran B, Tipparach U, Advanced Materials Research 741, 2013, 84.
- [13] U. Tipparach, P. Wongwanwatthana, T. Sompan, T. Saipin, and P. Krongkitsiri, CMU, J. Nat. Sci. Special Issue on Nanotechnology 7 (2008), 129.
- [14] Li, S., Y. Liu, G. Zhang, X. Zhao, J. Yin, Thin Solid Films. 520, 2011, 689.

- [15] Zuoli He, Wenxiu Que, Yucheng He, Jiaxing Hu, et al, Ceramics Int. 39, 2013, 5545.
- [16] Xiaobo Chen, Maria Schriver, Timothy S., Samuel S. M, Thin Solid Films 515, 2007, 8511.
- [17] Wanichaya Mekprasat, Wisanu Pecharapa, Energy Procedia 9, 2011, 509.
- [18] Dholam R, Patel N, Adami M, Miotello A., International Journal of Hydrogen Energy. 34(13), 2009, 5337.
- [19] N. A. Kelly, Thomas L. Gibson, International journal of hydrogen energy, 31, 2006, 1658.
- [20] L. X. Sang, Z. Y. Zhang, G. Bai, D. Chun, and M. Chong-fang, International journal of hydrogen energy, 37, 2012, 854.
- [21] P. Wongwanwattana, P. Krongkitsiri, P. Limsuwan, and U. Tipparach, Ceramics International 38S, 2012, S517.